TU/e EINDHOVEN UNIVERSITY OF TECHNOLOGY

Bond slip behaviour of deep mounted carbon fibre reinforced polymer strops confined with a ductile adhesive in clay brick masonry

Citation for published version (APA):
Türkmen, Ö. S., Wijte, S. N. M., & Vermeltfoort, A. T. (2018). Bond slip behaviour of deep mounted carbon fibre reinforced polymer strops confined with a ductile adhesive in clay brick masonry. In M. Masia, D. Alternam, Y. Totoev, & A. Page (Eds.), *Prtoceedings of the 10th Australasian Masonry Conference : Masonry Today and Tomorrow* (pp. 672-686)

Document status and date:
Published: 14/02/2018

Document Version:
Publisher's PDF, also known as Version of Record (includes final page, issue and volume numbers)

Please check the document version of this publication:

• A submitted manuscript is the version of the article upon submission and before peer-review. There can be important differences between the submitted version and the official published version of record. People interested in the research are advised to contact the author for the final version of the publication, or visit the DOI to the publisher's website.
• The final author version and the galley proof are versions of the publication after peer review.
• The final published version features the final layout of the paper including the volume, issue and page numbers.

Link to publication

General rights
Copyright and moral rights for the publications made accessible in the public portal are retained by the authors and/or other copyright owners and it is a condition of accessing publications that users recognise and abide by the legal requirements associated with these rights.

• Users may download and print one copy of any publication from the public portal for the purpose of private study or research.
• You may not further distribute the material or use it for any profit-making activity or commercial gain
• You may freely distribute the URL identifying the publication in the public portal.

If the publication is distributed under the terms of Article 25fa of the Dutch Copyright Act, indicated by the "Taverne" license above, please follow below link for the End User Agreement:

www.tue.nl/taverne

Take down policy
If you believe that this document breaches copyright please contact us at:

openaccess@tue.nl

providing details and we will investigate your claim.

Download date: 04. Aug. 2024

10TH AUSTRALASIAN MASONRY CONFERENCE

MASONRY TODAY AND TOMORROW

11 - 14 February, 2018
SYDNEY AUSTRALIA

www.10amc.com

BOND SLIP BEHAVIOUR OF DEEP MOUNTED CARBON FIBRE REINFORCED POLYMER STRIPS CONFINED WITH A DUCTILE ADHESIVE IN CLAY BRICK MASONRY

Ö. S. Türkmen[1], S.N.M. Wijte[2], J.M. Ingham[3] and A.T. Vermeltfoort[4]

[1] PhD Candidate, Department of the Built Environment, Section Structural Design, Eindhoven University of Technology, P.O. Box 513, 5600 MB, Eindhoven, the Netherlands, O.S.Turkmen@tue.nl

[2] Professor, Department of the Built Environment, Section Structural Designs, Eindhoven University of Technology, P.O. Box 513, 5600 MB, Eindhoven, the Netherlands, S.N.M.Wijte@tue.nl

[3] Professor, Department of Civil and Environmental Engineering, University of Auckland, 92019, Auckland, New Zealand, J.Ingham@auckland.ac.nz

[4] Associate Professor, Department of the Built Environment, Section Structural Design, Eindhoven University of Technology, P.O. Box 513, 5600 MB, Eindhoven, the Netherlands, A.T.Vermeltfoort@tue.nl

Retrofitting clay brick masonry using Deep Mounted (DM) Carbon Fibre Reinforced Polymer (CFRP) strips embedded in grooves filled with a ductile adhesive considerably increases the out-of-plane flexural capacity of slender unreinforced masonry walls. In order to investigate the bond-slip behaviour of CFRP-strips in a viscous-elastic adhesive, an extensive experimental program was initiated. Direct pull-out tests were conducted with clay brick masonry. Two parameters were investigated, namely, the type of adhesive (2 types) and the groove widths (10 and 15 mm). The second part of the experimental program focused on the pull-out capacity when surface treatment (primering or sandblasting) was applied to the CFRP-strips.

In literature dealing with bond behaviour the critical bond length was found using masonry prisms of approximately 350 mm in height. In the current study with CFRP strip application in conjunction with ductile epoxy, the critical bond length was not reached for specimens of nearly 1000 mm in length. This finding was an indication of a significantly improved stress distribution over the length of the embedded CFRP-strip as the appearance of peak stresses was prevented. No premature brick splitting was initiated despite the depth of the groove being 65% of the specimen thickness, whereas in literature this phenomenon was reported for groove depths of only 30%.

Keywords: *bond-slip, pull-out, masonry, reinforcement, seismic, retrofit, CFRP*

INTRODUCTION

In Groningen, an area in the North-East of the Netherlands, earthquakes occur as a result of the subsidence of the ground at relatively shallow depth beneath the earth's surface *(de Waal et al. 2015)*. This subsidence is caused by the extraction of gas from the Groningen gas field. As the majority of buildings in Groningen are composed of cavity walls with slender leaves of unreinforced clay brick masonry, and are designed to resist relatively moderate wind loads, it is essential to improve the earthquake resistance of the current buildings in the area to prevent collapse, with likely casualties. Due to the slenderness of the load bearing walls, the lateral load bearing capacity of these walls is mostly critical. Previous research has shown that retrofitting clay brick masonry with deep mounted (DM) Carbon Fibre Reinforced Polymer (CFRP) embedded in viscous-elastic adhesive, considerably increases the out-of-plane flexural capacity when compared to that of unreinforced masonry *(Türkmen et al. 2016, Türkmen et al. 2017, Wijte et al. 2017)*. DM is the same concept as the more widely known Near Surface Mounted (NSM) technique, except the CFRP strip is installed deep in the brick, so that the installed tensile component (CFRP) can provide additional flexural capacity and strength for both out-of-plane loading directions.

One of the recommendations following these aforementioned research projects was the necessity of more knowledge regarding the bond-slip behavior of the CFRP strips in the masonry, where the bond is created by embedding the strips in visco-elastic epoxy which is used as a groove filler. It is essential to quantify the interfacial bond-slip relation to allow for accurate modelling and understanding of debonding failures in FRP strengthened structures. There are several parameters that can influence this relation, such as the groove and the strip dimensions, the tensile and shear strength of the groove filler, and the position of the CFRP strip within the member being strengthened. The challenge is to find a suitable configuration at which the bond-slip behaviour provides sufficient flexibility to prevent masonry from premature cracking and results in high pull-out capacities in order to realise effective reinforcement.

The bond behaviour of CFRP systems can be experimentally studied with direct pull-out tests (DPT) and beam pull-out tests (BPT). Because the DPT method is less time consuming and cheaper to prepare and to undertake compared to the BPT test, this method was the starting point to find a configuration that led to the previously stated and desired bond slip behaviour.

SPECIMENS

The kiln fired clay bricks used this research had dimensions 205(±4)×97(±2)×49(±2) mm^3 (l×w×h) and had a normalized compressive strength of >15 MPa (manufacturer specs.). For the preparation of ±15L of mortar, 25 kg of M10 masonry mortar mix and 3.5L (±0.25) of water was used. The compression strength of the masonry prisms (14.81 MPa; COV 6.12%) was determined according to NEN-EN 772-1. The Young's modulus of the masonry was 3.1 GPa (COV 2.5%). Mortar prism flexural strength (3.56 MPa; COV 16.5%) and compressive strength (10.65 MPa; COV 20.7%) were determined according to EN-12390-5.

Compression tests carried out on samples extracted from existing masonry buildings show that the mean compressive strength and mean Young's modulus (coefficient of variation between brackets) are 12.7 (0.15) MPa and 9347 (0.27) MPa respectively for clay-solid masonry from before 1945,

and 17.7 (0.38) MPa and 9348 (0.35) MPa respectively for masonry from after 1945 *(Vermeltfoort. 2015)*. Thus the masonry used in the current research has a similar compression strength and a significant lower Young's modulus compared to the masonry in Groningen.

The prisms were constructed against a vertical sideboard to ensure minimum vertical deviation and were left to cure for at least 28 days. All masonry prisms consisted of 16 layers of brick in height and had typical mortar joint thicknesses of 13 mm. Even though various studies on pull-out behaviour of NSM FRP *(Willis et al. 2009; Dizhur et al. 2014)* approximate the critical bond length (and thus the required specimen height) as 100 times the FRP strip thickness, it was expected that this rule of thumb was not applicable in the current experimental program due to significant differences in the adhesive used. In order to prevent the specimens from being smaller than the critical bond length, a height of approximately 1000 mm for the prisms was selected.

Using a water cooled circular saw a groove was milled into the masonry prisms to depth d_f (Fig. 1). The dust in the groove was removed with compressed air. The CFRP strips (20×1.4 mm^2) were cleaned with acetone after cutting the strips into the specified length. If applicable, strain gauges (type PFL-10-11, foil strain gauges having polyester resin backing) were installed on alternating sides (to prevent asymmetric effects) at various locations with more frequent placement towards the loaded end (Fig. 2). The strain gauges were covered with wax to reduce the influence of the adhesive. A layer of primer was applied to the groove to obtain an improved bond of the applied adhesives to the masonry. Afterwards the CFRP strip was inserted into the groove that was partially filled with the flexible adhesive (type A or B) to a level exceeding d_{fs}. The CFRP strip was positioned centrally within the groove with a distance d_{fs}' of 10 mm from the bottom of the groove. The flexible adhesive exceeding d_{fs} was removed. Following the CFRP strip installation, the prisms were left to cure for one day before filling the remaining part (d_{ff}) of the groove with a conventional stiff adhesive. Afterwards another curing period of minimum seven days was maintained (stiff adhesive about 85% of end-strength). The relevant properties of the used flexible and stiff adhesives used, together with the properties of the CFRP strip are provided in Table 1.

Figure 1: Geometry of the groove and CFRP strip.

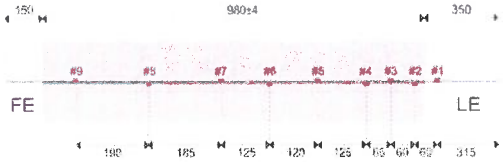

Figure 2: Pull-out specimen and the approximate positions of the strain gauges (indicated with #)

Table 1: Properties of the adhesive used (flexible and stiff) and CFRP

Component	Compressive strength [MPa]	Tensile strength [MPa]	E-modulus [MPa]	Elongation at break [%]	Poisson ratio [-]
Adhesive A	-	$5.5 \pm 0.2^{(1)}$	$34 \pm 0.5^{(1)}$	$89 \pm 8^{(1)}$	$0.48^{(2)}$
Adhesive B	-	$2.95 \pm 0.1^{(1)}$	$16.6 \pm 0.1^{(1)}$	$98 \pm 10^{(1)}$	$0.47^{(2)}$
CFRP	-	$\geq 2800^{(3)}$	$\geq 205{,}000^{(3)}$	$> 1.35^{(3)}$	-
Stiff adhesive	$45{,}5^{(4)}$	$6{,}5^{(4)}$	$26{,}000^{(5)}$	-	-

(1) Manufacturer specifications (M.S.) - DIN EN ISO 527 @ 200 mm/min; (2) M.S. - ISO 527 @ 10 mm/min; (3) M.S. - DIN EN 2561 @ 2 mm/min; (4) M.S. - DIN EN 12190; (5) M.S. - DIN EN 13412

Before the experiment, aluminium plates were glued to both sides of the CFRP strip at the loaded end using high strength instant adhesive. This procedure was a suggestion made by *Dizhur et al. (2014)* in order to facilitate a greater distribution of stress at the grips and thus prevent slippage.

METHODOLOGY

The experimental study for direct pull-tests consisted of two batches. The first batch for direct-pull-out tests consisted of specimens with two different adhesives (Table 2) and groove widths b_f (10 and 15 mm). Each configuration had two specimens from which only one had embedded strain gauges (SG). The CFRP strips had a smooth surface, which was denoted with "S" in the specimen coding. The goal with the first batch was to get more insight on the effect of the adhesive and groove dimensions on the pull-out behaviour of the embedded CFRP strips. The best (high pull-out strength and low corresponding slip) combination of adhesive (A) and groove width (10 mm) was used as standard for the remaining DPT's.

Table 2: Specimens for 1st batch

Spec.	Adh.	b_f (mm)	SG
A-S15-SG	A	15	Yes
A-S15	A	15	No
A-S10-SG	A	10	Yes
A-S10	A	10	No
B-S15-SG	B	15	Yes
B-S15	B	15	No
B-S10-SG	B	10	Yes
B-S10	B	10	No

Table 3: Specimens for 2nd batch

Spec.	Adh.(1)	Surface(2)	b_f (mm) (3)	SG
A-RP10-SG	A	RP	10	Yes
A-RP10	A	RP	10	No
A-SB10-SG	A	SB	10	Yes
A-SB10	A	SB	10	No

(1) Best performing adhesive 1st batch;
(2) RP = Roughened + primered; SB = Sand-blasted;
(3) Best performing groove width 1st batch

Because the failure of the best configuration of the first batch occurred at the CFRP and adhesive interface, additional pre-treatment of the CFRP was necessary to prevent this under-utilization of the strengthening system. A second batch was initiated to determine whether surface pre-treatment of the embedded CFRP strips would have a positive effect on the bond-slip behaviour. The surface treatment methods consisted of either adding a layer of primer after roughening the CFRP strips with sandpaper, or sand-blasting the CFRP strip. An overview of the tested specimens is provided in Table 3.

TEST SETUP

The direct pull-out tests were conducted on an Instron universal testing machine (Figure 3). The process started by carefully positioning the prism under the loading grips of the testing equipment, with the specimen resting on two support blocks. Hard cardboard was put on the top of the prism to prevent stress concentrations due to a possible non-flat surface of the brick. Afterwards the steel restrain plate on the loaded end was placed on top of the prism (Fig. 4). To prevent undesirable wedge type failure modes when using partial end restraint, a full restraint in the form of a 25 mm thick solid steel plate with three openings was selected. The centrally located opening allowed the loaded end of the CFRP strip to pass through. The smaller two openings allowed the LVDT's to rest on the specimen (Fig. 5). The specimen was then lifted up via the aluminium grip plates. This procedure made it possible for the prism to find its own balance point and thus minimize the eccentricity caused by imperfect installation of the CFRP strips. Using threaded rods, the steel restrain plate was bolted tight to the base of the installation until a pre tension force of 1.5 kN in the CFRP strip was monitored. After resetting the sensors, the experiment was started at a pull-out speed of 0.5 mm/min.

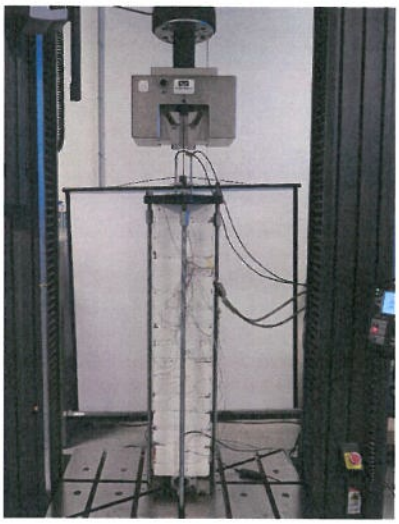

Figure 3: Experimental setup.

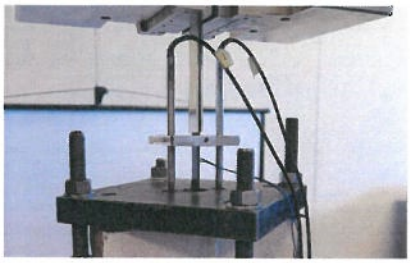

Figure 4: Detailed view of top support, loaded end LVDT's and aluminium plates.

Figure 5: Free end LVDT's.

Prior to the load application process, four LVDT sensors were installed. The upper two sensors measured the loaded end slip (Fig. 2) and the bottom two sensors measured the free end slip (Fig. 4). The mean of the two LVDT's was used to establish the corresponding slip. For the loaded end, the slip was corrected for the elongation over 70 mm of CFRP strip outside the specimen.

TEST RESULTS AND INTERPRETATION

The load-slip diagrams for the first batch of specimens are provided in Figs. 6-9. The abbreviations in the legend stand for loaded end slip (LE), which was corrected for the strain of the CFRP, and free end slip (FE). The notation (-SG) indicates the values for the specimen with embedded strain gauges. The regular specimens and the specimens with embedded strain gauges (-SG) are represented as blue and orange curves respectively. With the non-embedded strain gauges, the modulus of elasticity for the CFRP strip was determined for each experiment separately. The mean of the Young's modulus of the strips was found to be 196 GPa with a C.O.V. of 0.015.

For specimens A-S10(-SG), A-S15(-SG) and B-S10(-SG) with embedded strain gauges a clear decrease in pull-out capacity was observed. This finding was most likely caused by the reduced bonding area due to the placement of strain gauges. The test of specimen B-S15-S was disrupted because the edge of the component on which the free end LVDT's rested (Fig. 5), was clamped on one of threaded rods. This detail introduced an extra tensile force on the CFRP strip, which caused one of the FE LVDT's to fall out and the other one to malfunction. The clamping also explains the measured higher pull-out force measured for this specimen when compared to B-S15, despite the reduction in bond area due to the embedded strain gauges.

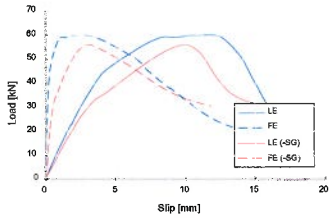

Figure 6: Load-slip diagram A-S10(-SG)

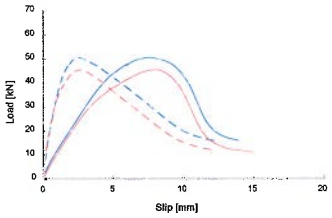

Figure 7: Load-slip diagram A-S15(-SG)

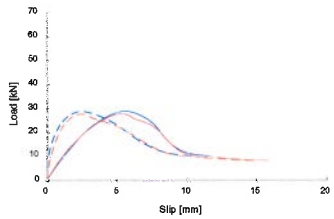

Figure 8: Load-slip diagram B-S10(-SG)

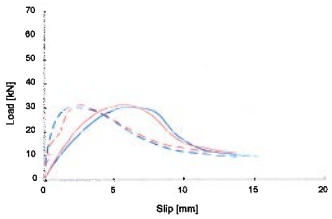

Figure 9: Load-slip diagram B-S15(-SG)

Fig. 10 shows the typical detachment of the CFRP strips from the adhesive, as was observed during these experiments. For all the specimens of this batch, a combined CFRP/adhesive interface failure and cohesive failure of the adhesive occurred. These findings indicated that improvements were

possible on the smooth CFRP strip surface in order to prevent CFRP/adhesive interface failure. With complete cohesive failure on the adhesive, a higher pull-out force was reached.

Despite a groove depth of 65 mm for all the specimens, premature brick splitting was not observed. Only specimen A-S10 developed some hairline cracks during the post-peak process around the CFRP and over the length of the specimen (Fig. 11). These cracks started developing after a 30% decline from the peak pull-out force, at a loaded end slip of 15 mm. For the remaining specimens no hairline crack development was observed. This observation was contradictory to the findings of *Dizhur et al. (2014)*, where pre-mature brick splitting was observed during the direct pull tests for specimens with a groove depth of only 30 mm. Based on the current findings, this premature failure mechanism was likely prevented with the application of a flexible adhesive instead of a stiff epoxy, as the more efficient confinement provided by the surrounding masonry is not the leading cause in premature failure prevention as observed by *Wijte et al. (2017)*.

Based on the load slip diagrams, it was concluded that adhesive A (higher tensile strength and Young's modulus) shows both a significantly higher bond energy (area under load-slip curve) and pull-out capacity than adhesive B. Additionally, a significant improvement of the pull-out capacity was realized when decreasing the groove width from 15 to 10 mm for adhesive A. This difference was not observed for adhesive B. Additional practical advantages of the smaller groove of 10 mm width are increased time-efficiency during installation and ~33% less material usage compared to the wider groove width of 15 mm. Due to these findings and observations, the combination of adhesive A and a groove width of 10 mm was the reference for the second batch of the experiments. The effects of an even smaller groove width than 10 mm were not investigated due to expected difficulties of milling such a small groove in the field.

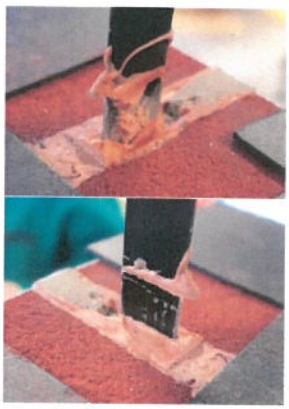

Figure 10: Typical view of loaded end after experiment 1st batch.

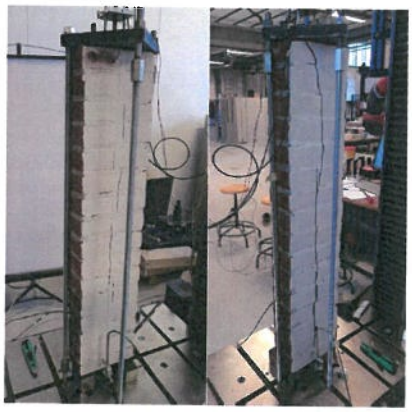

Figure 11: Marked hairline cracks during post-peak loading of the front (left) and back side (right).

The load-slip diagrams for the second batch of specimens are provided in Figs. 12 and 13. Comparing these diagrams with the load slip diagram of specimen(s) A-S10(-SG), an increase in

pull-out capacity of >10% was found. This finding indicated that both surface treatment methods provide a higher strength in terms of pull-out capacity to the smooth CFRP strip surface. This finding was also confirmed by the observed detachment of specimen A-RP10(-SG). Instead of a combined CFRP/adhesive interface and cohesive failure of the adhesive, cohesive failure becomes significantly more dominant (Fig. 14). For specimen A-SB10(-SG) the detachment was observed at the sand-layer/adhesive interface.

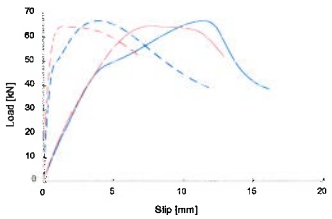

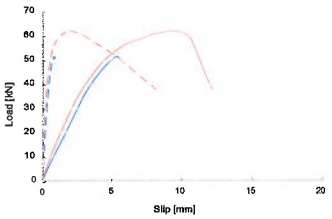

Figure 12: Load-slip diagram A-RP10(-SG) **Figure 13: Load-slip diagram A-SB10(-SG)**

The first test on specimen A-RP10 failed because the intended pull-out speed was not provided to the software, which resulted in the CFRP strip being pulled out significantly faster (>50 mm/min). The specimen failed at roughly 80 kN pull-out force after the tensile capacity of the CFRP was reached and the strip ruptured. This important accidental finding indicates that a higher pull-out speed has a significant influence on the bond of adhesive A.

Figure 14: Detachment of A-RP10.

Due to gripping problems, specimen A-SB10 slipped from the grips during the experiment. As the embedded region near the loaded end had most likely entered the post-peak region of the local bond-slip behaviour, the specimen was not tested again. Comparing both specimens with embedded strain gauges of this batch, it was observed that there was no significant difference in terms of pull-out capacity. Roughening the strip and adding a primer layer seemed to result in a slight increase in bond energy compared to a sandblasted strip. The former technique has an advantage in terms of application, because sanding the strip is more costly and time-consuming.

BOND DEVELOPMENT

To make a more detailed comparison between the performance of bond behaviour of the roughened/primered CFRP strip and the sandblasted CFRP strip, the development of the bond as a function of embedded length was analysed. In order to establish the local bond and slip behaviour using the embedded strain gauges, the following steps were applied. Based on the active strain gauges, a third order polynomial was constructed for the strain value over the entire embedded length for each moment of measurement (1 Hz). The location of the strain gauges installed over the embedded length of the CFRP strip is provided in Figure 2. Gauge #1 was an exception, because it was installed at the loaded end outside the masonry specimen.

The model was based on dividing the specimen into 980 elements of 1 mm length. For each element the decrease in tensile force in the embedded CFRP strips was approximated using Eq. (1). The decrease in tensile force is in equilibrium with the sum of the bond stress over the length and perimeter of the element (Eq. (2)). Combining equations (1) and (2) resulted in Eq. (3), with the assumption that the CFRP thickness was negligible compared to the width ($b_p + t_p \approx b_p$). Per element the local slip of the CFRP was calculated using the CFRP slip of the previous element, and the strain over the element (Eq. 4). The boundary condition was the slip before the first element (s_0), being the free end slip (s_{free}). Contrary to *Kashyap et al. (2012)* and *Dizhur et al. (2014)*, the calculations of the slip were based on the assumption that the axial strain in masonry and the slip at the unloaded end could not be neglected. Because of the significantly higher embedment length used in this research, the influence of the axial strain of the masonry needed to be taken into account. The tensile force in the strip is in equilibrium with the compression force in the masonry. When a uniform compression stress over the complete cross section of the specimen was assumed, Eq. 5 was found. The axial strain of the composite masonry was determined using the Young's modulus (Eq. 6). The total slip is the sum of the CFRP slip and the masonry axial strain (Eq. 7). To check whether the determined local bond and total slip was able to predict the experimental outcome, the sum of the shear forces of all the individual elements was compared to the measured pull force at the loaded end (Eq. (8)). Finally, the sum of the local slip (and the free end slip resulted in the theoretical loaded end slip (Eq. (9)).

(1)

(2)

(3)

(4)

(5)

(6)

(7)

(8)

(9)

(10)

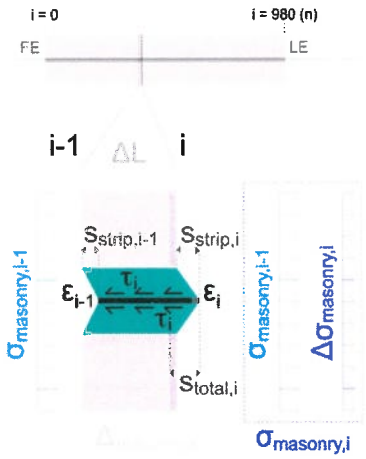

Figure 15: Typical view of loaded end after experiment 1st batch.

In order to check whether the proposed calculation steps were valid, a comparison was made between the experimental values and the theoretically calculated values for the pull-out capacity, LE slip and bond energy (Table 4). The comparison took place while the number of active strain gauges was 4 or more (as some strain gauges eventually fell out during the experiment). Looking at the difference in (Δ), no significant differences could be found for the pull-out capacity (<1.3%). The loaded end slip and bond energy showed slightly higher differences (<3.6% and <4.8% respectively), which was likely due to the deformation of the masonry.

Table 4: Experimental and theoretical comparison for pull-out capacity and bond energy.

Specimen	Pull-out capacity (kN)			Loaded end slip (mm)*			Bond energy (J)*		
	Exp.	Theo.	Δ (%)	Exp.	Theo.	Δ (%)	Exp.	Theo.	Δ (%)
A-S10-SG	56.00	56.11	+0.20	12.41	12.38	-0.27	485	490	+1.2
A-S15-SG	45.37	45.26	-0.25	9.70	9.50	+2.05	313	311	-0.4
B-S10-SG	27.57	27.80	+0.81	5.69	5.89	+3.60	105	109	+3.8
B-S15-SG	31.26	31.46	+0.62	7.84	7.88	+0.45	183	178	-2.4
A-RP10-SG	64.47	65.25	+1.26	8.75	8.97	+2.53	392	410	+4.8
A-SB10-SG	62.28	62.57	+0.45	10.65	10.88	+2.22	495	514	+3.9

* Until the moment where 4 or more strain gauges were active.

In order to compare the results for the bond behaviour obtained from the different DPT experiments in a time-efficient way, a graphical representation of the local bond development was proposed in the form of a contour plot. The development of the local bond over the length as a function of the loaded end slip is provided in Figure 16 for specimen A-RP10-SG. The same figure also shows the pull-out force (white) as a function of the loaded end slip.

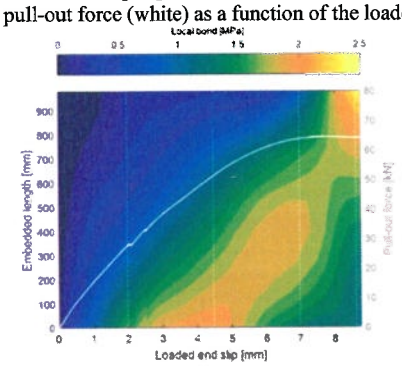

Figure 16. Contour plot of the local bond over the embedded length (coloured) and the pull-out force (white) as a function of the LE slip for A-RP10-SG.

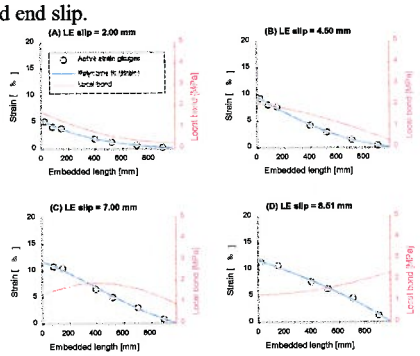

Figure 17. The active strain gauges, the polynome of the strain, and the local bond as a function of the embedded length at four different LE slips for A-RP10-SG.

In order to explain how this figure was obtained and how it should be interpreted, four different moments (indicated with the dashed vertical lines in Fig. 16) are discussed in more detail using Figure 17. At a loaded end slip of 2.00 mm (Fig. 17a) first a polynome for the strain over the embedded length was constructed (blue curve) using the active strain gauges (black circles). Using the previously explained calculation steps, the local bond over the embedded length (orange curve) can be determined. This distribution of the local bond was represented with the vertical color development at 2 mm LE slip value for the x-axis. Here it can be seen that quite early in the process, far before reaching the maximum value for local bond at the loaded end (roughly 2.0 MPa), the adhesive was activated over the entire embedded length. This observation indicates that the embedded length of nearly 1000 mm in this research was shorter than the critical bond length. Because the LE slip increased to 4.5 mm, not only does the area near the loaded end approximate

the maximum value, but the loaded end also starts to get activated more (Fig. 17b). This development can clearly be seen looking at the the region 2.0 mm < LE slip < 4.5 mm in Fig. 16. Further increasing the LE slip initiates the post-peak process in the near-loaded end area, and moves the stresses more towards the free end (Fig 17c/d). This phenomna is indicated by the shift of the yellowish area from the LE towards the FE between 4.0 mm and 8.5 mm LE slip in Fig. 16.

Looking at the calculated free end slip (7.95 mm) at the moment when the maximum pull-out force is reached for A-RP10-SG, the slip of the CFRP itself accounts for 93.4% (7.42 mm) of the total slip according to the model. This finding means that the axial strain of the masonry of 0.52 mm (6.6%) due to compression cannot be neglected during modelling.

Fig. 18a and 18b present the contour plots of the developing bond for specimens SB10-SG and S10-SG respectively. When compared with A-RP10-SG, specimens SB10-SG and S10-SG show a strong decrease of the local bond towards the loaded end, at an LE slip of about 7 mm. The dark blue regions indicate complete detachment, while for A-RP10-SG the local bond remains approximately 1.2 MPa as can be seen in Fig. 16. From the analysis it can be stated that roughening the strips and adding a primer layer seemed to evoke a significantly better post-peak behaviour when compared to the alternatives with sand-blasting or without surface treatment.

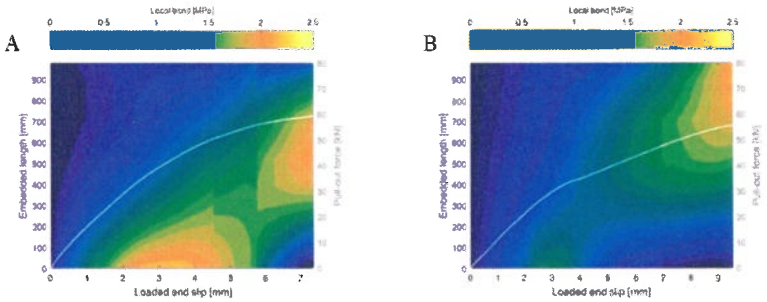

Figure 18. Contour plot of the local bond over the embedded length (coloured) and the pull-out force (white) as a function of the LE slip time for A-SB10-SG (A) and A-S10-SG (B).

COMPARISON WITH PREVIOUS RESEARCH

Looking at the database of all 82 NSM CFRP strips-to-masonry pull tests available in the open literature, the minimum value of the Young's modulus for the applied adhesives is found to be 2,000 MPa *(Seracino et al 2007; Konthesinga et al 2009; Petersen et al. 2009; Willis et al 2009; Kashyap et al. 2012; Dizhur et al 2014)*. Adhesive A, which has shown the best performance in the reported study, has a Young's Modulus of only 34 MPa (nearly a factor of 60 lower).

In order to show the siginificant difference in bond behaviour when applying a ductile adhesive instead of a conventional stiff epoxy, as a final step the performance of A-RP10-SG was compared to specimen B1-4-15-(6/20) tested by *Dizhur et al. (2014)* . Although the two specimens are not

equal in terms of masonry properties and groove/CFRP geometry, this difference has no significant influence on the main objective of comparing the performance of the adhesives. Fig. 19 shows this comparison in the form of bond over the embedded length at the moment of maximum pull-out force. Where a conventional adhesive shows bond concentrations over a limited embedment length (peak around 9.5 MPa), the flexible adhesive used in the reported study shows a nearly uniform distribution (varying between 1-2 MPa). In contrast to the existing database of DPT tests of CFRP on masonry, this observation is the primary factor why no intermediate cracking was observed in this research.

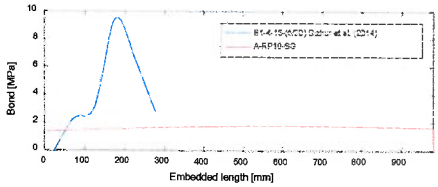

Figure 19. Bond over embedded length at maximum pull-out force for B1-4-15-(6/20) Dizhur et al. (2014) and A-RP10-SG

CONCLUSIONS

Direct pull-out tests were conducted with different flexible adhesives, groove widths and surface treatment configurations. The conclusions of the conducted research were:

1. Adhesive A (higher tensile strength and Young's modulus) performed significantly better than adhesive B for the performed DPT's, both in terms of bond energy and pull-out capacity.
2. Narrowing the groove width from 15 mm to 10 mm led to a higher bond-energy and pull-out capacity for adhesive A.
3. Despite a groove depth of 65% of the brick thickness, no premature cracking was observed. In comparable research with conventional adhesive it was observed that intermediate cracking was the leading failure mechanism at groove depths of only 30%
4. Adding a primer layer to the CFRP strip resulted in a higher pull-out capacity, as the partial CFRP/adhesive interface failure was shifted to a full cohesive failure of the adhesive. The same finding was also applicable for sand-blasted strips.
5. Analysing the bond development showed that roughening the CFRP strip and adding a primer layer not only improved the bond strength, but also advanced the post-peak behaviour when compared to the situation with no surface treatment or sand-blasted surface.
6. Adhesive A used in this study showed a near uniform distribution (1-2 MPa) over an embedded length of approximately 980 mm, where conventional adhesive showed bond concentrations (peak around 9.5 MPa) over a limited embedment length of < 300 mm).
7. Adhesive A used in this study has a significantly lower (factor 60) Young's modulus when compared to the values for the modulus of elasticity found for the used adhesive in the database of all 82 previously conducted NSM CFRP strip-to-masonry pull tests (> 2,000 MPa).
8. The critical bond length for adhesive A was not reached for a 980 mm anchorage length.

9. Contrary to previous research, the axial strain of the masonry could not be neglected when applying a flexible adhesive, as the bond length was significantly higher.
10. The speed at which the DPT was conducted had a major influence on the bond behaviour for adhesive A, as it was found that the adhesive behaves stronger and stiffer.
11. A graphical representation of the local bond development over time was proposed in the form of a contour plot, so that the results from the different DPT experiments could be compared in a time-efficient way for the bond behaviour.

RECOMMENDATIONS

The first recommendation in order to get more insight on the bond slip behaviour of DM CFRP strips confined with a ductile adhesive in clay brick masonry is to conduct more DPT's where the pull-out speed is varied. Secondly, LVDT's should be installed over the height of the masonry specimens to determine the axial strain during the experiment, because the influence of this parameter cannot be neglected. Thirdly, BPT's should be conducted in order to also take flexural behaviour into account. Fourthly, cyclic loads should be applied to investigate degradation effects. Finally, both FE and mechanical models should be developed for engineering purposes.

ACKNOWLEDGEMENTS

The authors wish to thank and acknowledge Royal Oosterhof Holman and SealteQ Group for supporting this research into the behaviour of CFRP reinforcement with ductile adhesive.

REFERENCES

de Waal, J. A., Muntendam-Bos, A. G., and Roest, J. P. A. (2015). Production induced subsidence and seismicity in the Groningen gas field – can it be managed? Proc. IAHS, 372, 129-139.

Türkmen, Ö.S., Vermeltfoort, A.T. and Martens, D.R.W. (2016). Seismic retrofit system for single leaf masonry buildings in Groningen. Proceedings of 16th International Brick and Block Masonry Conference, June 27-29, Padova, Italy.

Türkmen, Ö.S., Vermeltfoort, A.T., Wijte, S.N.M., Martens, D.R.W. (2017). Experiments to determine the out of plane behaviour of CFRP and ductile adhesive reinforced clay brick masonry walls. Proceedings of 13th Canadian Masonry Symposium, June 4-7, Halifax, Canada.

Wijte, S.N.M., Türkmen, Ö.S., Vermeltfoort, A.T., Martens, D.R.W. (2017). Analytical modelling of the out of plane behaviour of CFRP and ductile adhesive reinforced clay brick masonry walls. Proceedings of 13th Canadian Masonry Symposium, June 4-7, Halifax, Canada.

Vermeltfoort, A.T. (2015). Tests for the characterization of original Groningen masonry under compression and shear loading, Eindhoven University of Technology.

Willis, C.R., Yang, Q., Seracino, R., Griffith MC. (2009). Damaged masonry walls in two-way bending retrofitted with vertical FRP strips. Constr Build Mater; 23:1591–604.

Dizhur, D., Griffith, M.C., Ingham, J.M. (2014). Pullout strength of NSM CFRP strips bonded to vintage clay brick masonry. Engineering Structures, Volume 69, pp. 25-36

International Organization for Standardization (2012). Plastics - Determination of tensile properties. DIN EN ISO 527.

International Organization for Standardization (1995). Aerospace series - Carbon fibre reinforced plastics - Unidirectional laminates - Tensile test parallel to the fibre direction. DIN EN 2561.

German Institute for Standardization (1998). Products and systems for the protection and repair of concrete structures - Test methods - Determination of compressive strength of repair mortar. DIN EN 12190.

German Institute for Standardization (2006). Products and systems for the protection and repair of concrete structures - Test methods - Determination of modulus of elasticity in compression. DIN EN 13412.

Kashyap, J., Willis, C.R., Griffith, M.C., Ingham, J.M., Masia, M.J. (2012). Debonding resistance of FRP-to-clay brick masonry joints, Engineering Structures, Volume 41, pp. 186-198

Seracino, R., Jones, N.M., Ali, M.S.M., Page, M.W., Oehlers, D.J. (2007). Bond strength of near surface mounted FRP strip-to-concrete joints. J Compos Constr;11:401–9.

Konthesingha, K.M.C., Masia, M.J., Petersen, R.B., Page, A.W. Bond behaviour of NSM FRP strips to modern clay brick masonry prisms under cyclic loading (2009). 11th Canadian masonry symposium. Toronto, Canada: McMaster University/Canadian Masonry Design Centre; p. 665–74

Petersen, R.B., Masia, M.J., Seracino, R. (2009). Bond behaviour of near-surface mounted FRP strips bonded to modern clay brick masonry prisms: influence of strip orientation and compression perpendicular to the strip. J Compos Constr;13:169–78.